Steel and Composite Structures, *Vol. 36, No. 4* (*2020*) *383-398*
DOI: https://doi.org/10.12989/scs.2020.36.4.383

Progressive collapse of steel-framed gravity buildings under parametric fires

Jian Jiang[1], Wenyu Cai*[2], Guo-Qiang Li[2], Wei Chen[1] and Jihong Ye[1]

[1]*Jiangsu Key Laboratory of Environmental Impact and Structural Safety in Engineering, China University of Mining and Technology, Xuzhou 221116, China*
[2]*College of Civil Engineering, Tongji University, Shanghai 200092, China*

(*Received December 9, 2019, Revised July 18, 2020, Accepted July 24, 2020*)

Abstract. This paper investigates the progressive collapse behavior of 3D steel-framed gravity buildings under fires with a cooling phase. The effect of fire protections and bracing systems on whether, how, and when a gravity building collapses is studied. It is found that whether a building collapses or not depends on the duration of the heating phase, and it may withstand a "short-hot" fire, but collapses under a mild fire or a "long-cool" fire. The collapse time can be conservatively determined by the time when the temperature of steel columns reaches a critical temperature of 550 °C. It is also found that the application of a higher level of fire protection may prevent the collapse of a building, but may also lead to its collapse in the cooling phase due to the delayed temperature increment in the heated members. The tensile membrane action in a heated slab can be resisted by a tensile ring around its perimeter or by tensile yielding lines extended to the edge of the frame. It is recommended for practical design that hat bracing systems should be arranged on the whole top floor, and a combination of perimeter and internal vertical bracing systems be used to mitigate the fire-induced collapse of gravity buildings. It is also suggested that beam-to-column connections should be designed to resist high tensile forces (up to yielding force) during the cooling phase of a fire.

Keywords: progressive collapse; gravity building; parametric fire; cooling phase; fire protection; bracing system

1. Introduction

The traditional way of determining fire resistance of a structure is to test its critical members in a standard fire (e.g. ISO 834 fire). Such tests are conducted in a furnace (with a dimension smaller than 5 m) on simply supported members with a failure criterion of either failure of the member, limit of deformation, rate of deformation or limiting temperature. Since the Broadgate Phase 8 fire and the subsequent Cardington fire tests (Kirby 1997) in the 1990s, the global behavior of steel framed structures in fire has received growing concern (Shahabi *et al.* 2016; Ye *et al*. 2019). It has been confirmed that steel members in real multi-story buildings have significantly greater fire resistance than isolated members in standard fire tests, mainly due to the realistic member dimension, boundary restraint, and fire scenario. From then on, the research focus moves from simply supported structural members to restrained members (Pantousa *et al.* 2017, Davoodnabi *et al.* 2019, Lim *et al.* 2019).

Especially since the collapse of Word Trade Tower (WTC) under the terrorist attack on September 11, 2001, there have been growing interests in understanding progressive (or disproportionate) collapse behavior of structures under accidental loads such as blast, impact or fire (Menchel *et al.* 2009, Tian *et al*. 2017, Huang *et al.* 2019, Ferraioli 2019). The term "progressive collapse" is defined as "the spread of an initial local failure from element to element, eventually resulting in the collapse of an entire structure or a disproportionately large part of it" (ASCE 2005). It implies that large displacements, even failure, of individual structural members are acceptable given the prevention of global structural collapse. An important lesson from the collapse of WTC is that prescriptive fire resistance ratings of individual structural members do not guarantee the adequate performance of a whole building system (Cowlard *et al.* 2013). The term "fire resistance rating" is associated with the ability of a building element to perform its function as a barrier or structural component for a specified time during the course of a fire. Since then, the research focus further moves to the global collapse behavior of buildings under fire conditions and performance-based design for structures in fire (Cesarek *et al.* 2018).

The commonly used approaches such as alternate path method as specified in various design codes (DoD 2010, GSA 2003, Kim and Park 2008, Stevens *et al.* 2011) are more applicable to blast or impact rather than fire effects, although they are typically considered to be "threat independent" (Mirtaheri and Zoghi 2016). Firstly, the duration of fire (in hour) is much longer than that of blast (in millisecond), and thus the behavior of structures exposed to fire is a quasi-static process until approaching the failure state of heated members (Richard Liew and Chen 2004). Secondly, the time when a structure collapses (i.e., fire resistance) is a key factor apart from whether it collapses. This fire resistance against structural collapse

*Corresponding author, Ph.D.
E-mail: wenyucai@tongji.edu.cn

ISSN: 1229-9367 (Print), 1598-6233 (Online)

depends on the failure process of heated members which should be explicitly simulated in numerical models, instead of being removed in alternate path method. In addition, only one column is removed each time in the alternate path method compared to several members simultaneously heated in the case of fire (Rezvani *et al*. 2017). This means that the local failure of all heated elements should be included in the structural analysis of buildings exposed to fire to ensure an accurate prediction of both collapse time and collapse mode. Therefore, more efforts should be put in investigating the fire-induced collapse of structures, focusing on whether, how and when a structure collapses in fire.

The early studies on fire-induced collapse of structures focus on their collapse mechanism and corresponding influencing factors such as load ratio, strength of beams, columns, connections and slabs, fire scenario, and fire protections. A comprehensive review on these studies can be found in the references (Porcari *et al.* 2015, Jiang and Li 2018). Three collapse modes of steel framed buildings have been found, including general collapse mode, lateral drift collapse mode, and global downward collapse mode (Jiang and Li 2018). The general collapse mode is the most common collapse mechanism where the collapse is due to the buckling of adjacent columns experiencing obvious lateral drift (Fang *et al*. 2012, Jiang and Li 2017a). When the catenary action in the beam is significant or the load ratio is high, the lateral drift of the structure will govern its collapse (Ali *et al*. 2004, Sun *et al.* 2012), resulting in a lateral drift collapse mode. If the lateral drift of the frame is restrained, it will globally collapse downward such as in the cases of strong beams, high load ratios or multi-compartment fires (Jiang and Li 2017).

These previous studies have four main issues: (1) many previous studies focus on two-dimensional (2D) frames rather than three-dimensional (3D) frames. The 2D models cannot consider the effect of slabs through tensile membrane action (Yu *et al*. 2010, Alashker *et al.* 2010, Pham and Tan 2013) and the realistic load redistribution path (Ma and Richard Liew 2004, Flint *et al.* 2007). A comparison between 2D and 3D models (Jiang and Li 2017b) showed that 2D models produced conservative results by underestimating the collapse resistance, and the load redistribution in a 2D model cannot be captured as in a 3D model where more loads were redistributed along the short span than those along the long span; (2) most previous studies were conducted based on small compartment fires with a heating phase alone (i.e., standard fires), rather than small compartment fires with a cooling phase (e.g., parametric fire), large compartment fires (e.g. localized fire) and spread of fires (e.g., travelling fire). A review on the effect of fire scenarios is presented below; (3) most previous studies focus on moment-resisting frames rather than gravity frames. This is largely because of the easiness in numerical simulation of rigid connections rather than pinned or semi-rigid connections. NIST research (Sadek *et al*. 2008) has demonstrated the vulnerability of steel gravity framing systems with shear connections to disproportionate collapse under column loss scenarios, while seismically designed moment-resisting frames have been shown to be robust against column loss in previous experimental and computational studies by NIST (Sadek *et al.* 2010); (4) most previous studies deal with collapse modes rather than measures to mitigate or prevent structural collapse. The objective of this paper is to investigate the collapse behavior of 3D gravity frames under realistic fires with a cooling phase, and to propose effective mitigation measures for practical structural fire design.

Standard fire curves such as ISO 834 or ASTM E119 fires represent only the fully developed phase of a fire which is considered as the worst-case fire in enclosure. It is evident that they cannot exhibit the behavior of a realistic fire which includes its four phases of ignition, growth, full development, and decay. To better represent a realistic fire, natural fire curves (or parametric fire) are developed by taking into account the geometry of the compartment, ventilation condition, fire load density, thermal characteristics of boundary materials. The primary difference between standard and natural fire curves is that the latter account for a cooling phase. It was found that a frame may collapse in the cooling phase in the high-ventilation fire due to the less rapid temperature rise in the column than the beam because of the large cross-section of the column (Lien *et al.* 2009). Neal *et al*. (2012) pointed out that the fire type (standard or natural fires) had negligible effect on the collapse behavior of unprotected frame since unprotected members failed at the early stage of a fire where the temperature time history is similar for different fire types. For protected frames, the natural fire with a decay phase could lead to a longer fire resistance. However, most of these studies on the cooling phase of a fire are either on structural members or 2D frames. It is therefore necessary to further investigate the effect of the cooling phase on the global behavior of structures.

This paper numerically investigated the fire-induced progressive collapse of three-dimensional steel-framed gravity buildings. A 10-storey gravity building with reinforced concrete slabs was designed and analyzed for three realistic fire scenarios with a cooling phase, representing “short-hot”, mild, and “long-cool” fires, respectively. The effect of mitigation measures such as increasing fire protection levels and application of bracing systems was investigated. The impact of slabs and connections on the collapse behavior was also studied. Recommendations for practical design were proposed to enhance the collapse resistance of gravity buildings due to fire effects.

2. Modeling of the prototype building

2.1 Design of the prototype building

For simplicity of analysis, a multi-story steel framed gravity building published by NIST (Main and Sadek 2012) was selected as the prototype structure. The layout of the prototype building is shown in Fig. 1. It is a 10-story, 5-bay frame representative of a typical office building with a rectangular plan dimension of 45 m × 30 m. The building was designed for Seismic Design Category C (ASCE 2005),

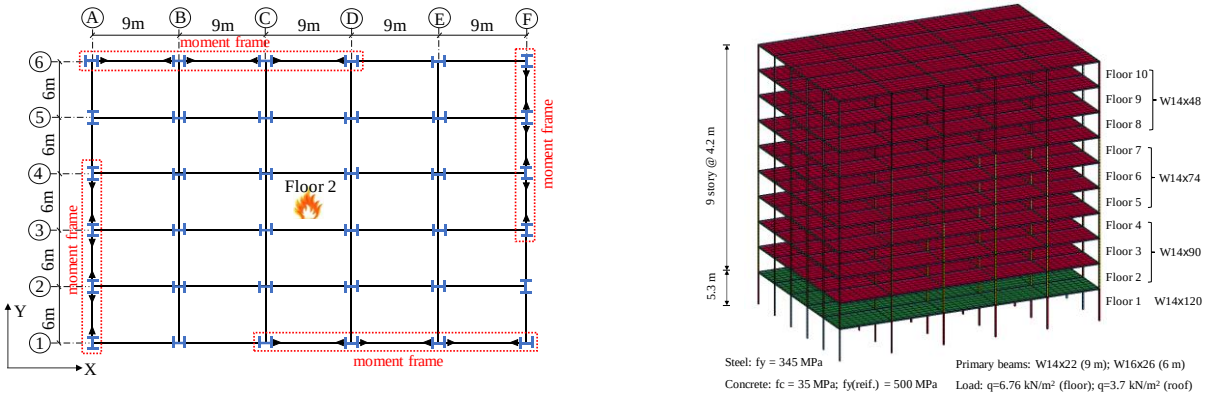

Fig. 1 Modeling of a 3D 10-storey prototype building: (a) plan view and (b) finite element model

and the lateral loads are resisted by seismically designed intermediate moment frames (IMFs) located on the exterior of the building (rigid beam-to-column connections were used). Pinned beam-to-column connections were used for all interior frames which were designed to sustain gravity loads only. The length of each bay along X and Y direction is 9 m and 6 m, respectively. The height of the ground floor and upper floors is 5.3 m and 4.2 m, respectively. The primary beams with a span of 9 m and 6 m have a cross section of W14×22 and W16×26, respectively. The cross section of the columns on the floor 1, floors 2-4, floors 5-7, and floors 8-10 is W14×120, W14×90, W14×74, and W14×48, respectively. The Young's modulus and yield strength of steel members are 200 GPa and 345 MPa, respectively. Note that the steel grade does affect the collapse behavior of structures, in both beneficial and detrimental ways. Use of high-strength steels is beneficial for increasing the collapse safety margin of structures, but high-strength steels may experience greater degradation of material properties and less ductility at elevated temperatures. Therefore, the findings in this study are applicable to normal-strength steel structures, and it is necessary to further investigate the collapse behavior of high-strength steel structures.

To overcome the difficulty in simulating the profiled composite slabs with steel decking by shell elements (Huang *et al.* 2000, Izzuddin *et al.* 2004), flat reinforced concrete slabs with a thickness of 120 mm were simulated in the model to equivalently represent the composite slabs used in the original design. The reinforcement has a diameter of 12 mm and spacing of 200 mm, with a reinforcement ratio of 0.5 % and area of steel per meter of 565 mm^2/m. The concrete cover of reinforcement bars is 30 mm from the bottom of the slab. The compressive strength of concrete is 35 MPa, and the yield strength of reinforcement is 500 MPa.

The design dead and live loads of the floors are 3.64 kN/m^2 and 4.79 kN/m^2, respectively. For the roof, they are 2.68 kN/m^2 and 0.96 kN/m^2, respectively. The load combination of $1.2D + 0.5L$ at the fire limit state (ASCE 2005) was used, where D is the dead load and L is the live load. Thus, the calculated uniformly distributed loads are 6.76 kN/m^2 and 3.7 kN/m^2 imposed on the floors and roof, respectively. In this study, the load ratio of a structural member is defined as the ratio of the imposed load to its ultimate load-bearing capacity. The ultimate capacities of the members (beams, columns, slabs) were directly determined from the numerical model by loading them until failure. This is to reflect their realistic capacity by considering the realistic boundary conditions. It was found that the ultimate capacities of the four types of columns from the bottom floor to the top floor were 7800 kN, 5820 kN, 4770 kN, 3080 kN, respectively. The internal gravity columns on floor 1, floor 2-4, floor 5-7, floor 8-10 have load ratios of 0.45, 0.41-0.54, 0.27-0.42, 0.06-0.3, respectively. The load ratio of the 9m and 6m composite beams is 0.29 and 0.25, respectively. The slabs have a load ratio of 0.27.

2.2 Numerical model of the prototype building

A 3D numerical model of the prototype building was created in finite element software LS-DYNA, as shown in Fig. 1(b). The steel columns and beams were simulated by three-dimensional Hughes Liu beam elements. The Hughes-Liu beam element is developed based on a degeneration of the isoparametric 8-node solid element (Hughes and Liu 1981). The local buckling of structural members cannot be simulated by this element (only global buckling was considered). This element has an integrated cross-section and the command *INTEGRATION_BEAM was used to define an I-shape section.

Table 1 Cross sections of structural members in the prototype building

Floor level	Story height	Beam		Column
		9 m	6 m	
1	5.3 m	W14×22	W16×26	W14×120
2-4	4.2 m	W14×22	W16×26	W14×90
5-7	4.2 m	W14×22	W16×26	W14×74
8-10	4.2 m	W14×22	W16×26	W14×48

The arrangement of the integration points is achieved by an integration refinement parameter k. A value of k=2 was taken in this study where 7 and 6 integration points were arranged for the flange and web, respectively. An initial imperfection of *length*/1000 was imposed on columns.

The slabs were modeled by a layered composite shell formulation (*PART_COMPOSITE) in which a distinct structural material, thermal material, and thickness can be specified for each layer. This allows distinct layers to be specified for the reinforcement and concrete through the thickness of the slab. The steel beam shared the same node with the slab to form a composite beam with a rigid connection between the slab and beam. Pinned beam-to-column connections were simulated by releasing the rotational degree of freedom at the end of the beams in the command *ELEMENT_BEAM. The MAT_202 (MAT_Steel_EC3) was used for steel beams and columns at ambient and elevated temperatures. The temperature-dependent material properties of steel refer to CEN (2005). The material MAT_172 (MAT_CONCRETE_EC2) was used to model the reinforced concrete slab at ambient and elevated temperatures. The stress-strain curves in this material for the concrete and reinforcement at ambient and elevated temperature are as specified in CEN (2004).

An explicit dynamic analysis was carried out instead of implicit analysis to overcome its convergence problems. The implicit analysis needs iterative solution process for each time step, and has convergence problems when calculating inverse of the structural stiffness matrix. The explicit analysis avoids iterations but requires extremely small time steps to ensure a stable and accurate prediction, which costs huge computing time. To save the computation cost, a time-scale technique was used for explicit analysis to scale the real heating duration in hours down to a simulation time in seconds. The "simulation time" is the time written in the program code to represent the rate of temperature variation. Experimental results (Jiang *et al.* 2016, 2018) showed that the response of restrained steel columns under fire may be quasi-static or dynamic, depending on the restraint condition, load ratio and column slenderness. The time scaling may affect these two responses. Sensitivity analyses were carried out on two column tests and three slab tests (at ambient and elevated temperature) (Jiang *et al.* 2016, Jiang and Li 2017a, Jiang *et al.* 2020) to determine and validate the appropriate time scale for modeling steel framed structures in LS-DYNA. For quasi-static responses, the time scale can be determined as long as the loads and the temperature variations are applied sufficiently slowly that spurious dynamic effects are not introduced. For dynamic responses, the time scale factor can be selected when a similar maximum axial displacement at the top of buckled columns is predicted compared to the measured value. The validation indicates that it is feasible to scale down the hours-long fire duration to a simulation time of seconds in an explicit dynamic analysis, without adversely affecting the accuracy of the results. Note that this finding is applicable to a standard fire (e.g., ISO 834) which only has a heating phase. In this study, a simulation time of 8 seconds was used instead of a real time of one hour, i.e., a time scale factor of (3600s)/(8s) = 450. More details were presented in Section 2.4. It can not only significantly save the computing time but simulate the quasi-static and dynamic effects on the remaining structures due to sudden local failure.

2.3 Design of fire scenarios

It was assumed that a fire occurred in an interior compartment on Floor 2 since the internal columns on this floor have the highest load ratio. This assumption is not a realistic case since a fire on lower floors can be easily extinguished by firefighters before causing structural collapse. However, from the view of similarity in collapse mechanism, such a lower-floor fire scenario was selected for a 10-storey building in this study to represent a typical fire scenario on upper floors (e.g., > 5th floor) for a taller high-rise building. Based on the typical compartment size of 9 m×6 m×4.2 m on Floor 2, three parametric fires with a cooling phase were chosen in this study, as shown in Fig. 2. The parametric temperature-time curves of these fires were calculated according to Annex A of EN1991-1-2 (CEN 2002), depending on the fire load density ($q_{t,d}$), enclosure property (b) and opening factor (O). The fire load density represents the combustibility of the fuel in the compartment, the enclosure property represents the speed of heat loss from the walls of the compartment, and the opening factor denotes the ventilation condition in the compartment. A value of $q_{t,d}$ =800 MJ/m^2 and b=1160 J/m^{2}s$^{1/2}$K were used which were determined based on the compartment size of the building and typical materials used in building construction. The three cases (Fire 1, Fire 2, Fire 3) have different opening factors of 0.08, 0.04, and 0.02, representing "short-hot" fire, mild fire, and "long-cool" fires, respectively. The "short-hot" fire is a fire reaching a high temperature in a short time (less than 30 min), while the "long-cool" fire lasts for a longer time with a relatively lower maximum temperature (total duration of more than 6 hour).

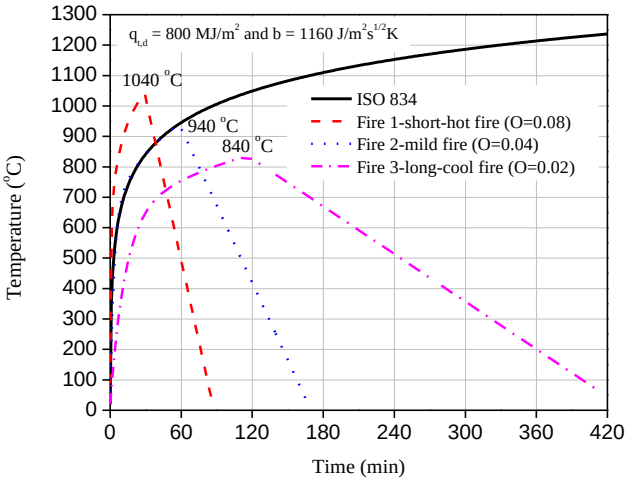

Fig. 2 Parametric temperature-time curves for fire simulation of the building

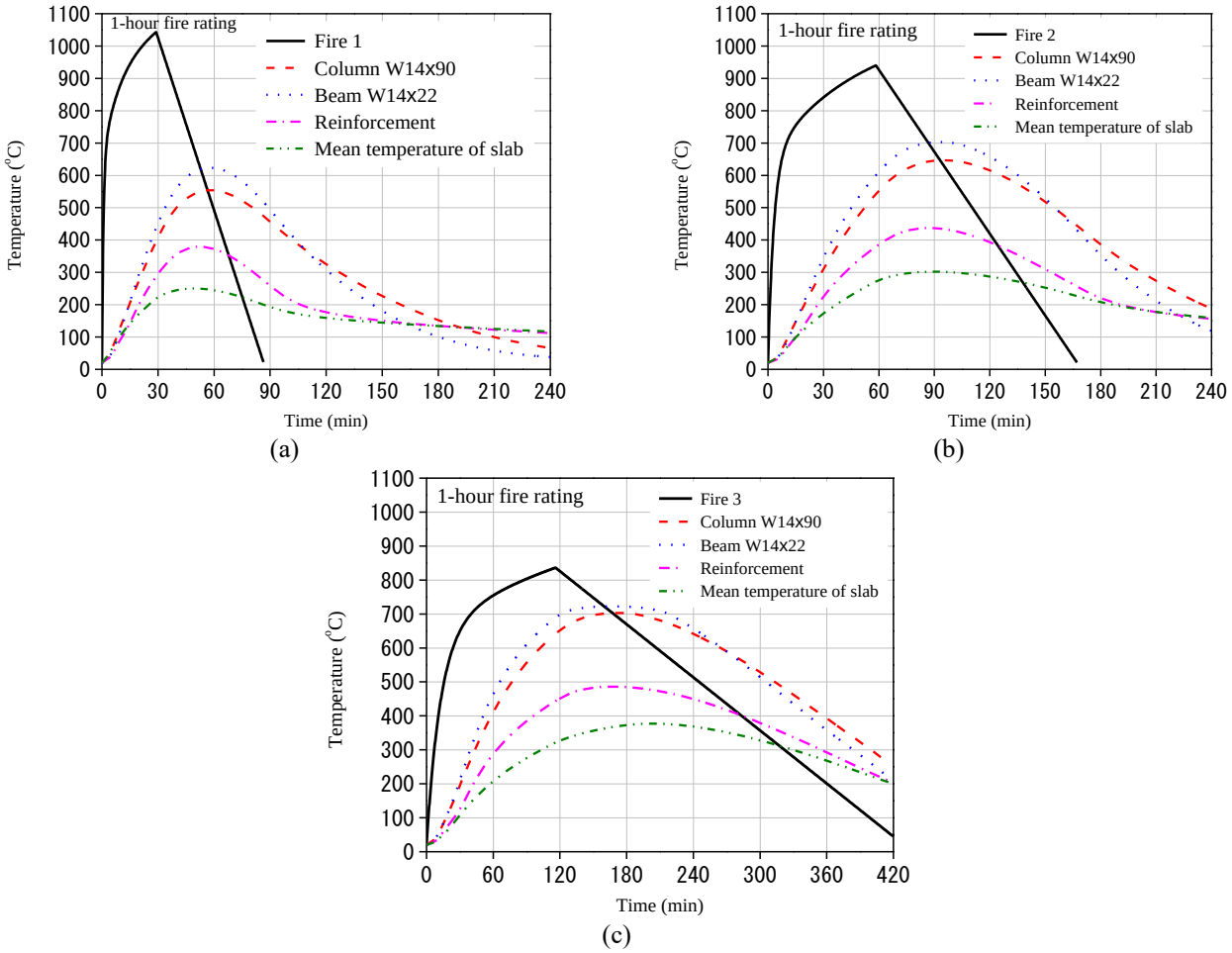

Fig. 3 Temperature-time curves of steel and concrete members for 1-hour fire-resistance rating: (a) Fire 1, (b) Fi re 2 and (c) Fire 3

Table 2 Key parameters of fire curves and temperature of structural elements

Fire case	Temperature of gas			Temperature of structural members					
				Column		Beam		Reinforcement	
	T_{max} (°C)	t_{max} (min)	t_u (min)	T_{max} (°C)	t_{max} (min)	T_{max} (°C)	t_{max} (min)	T_{max} (°C)	t_{max} (min)
Fire 1	1040	30	90	555	57	626	57	380	52
Fire 2	940	60	165	646	93	700	90	436	87
Fire 3	840	120	420	700	168	725	162	487	160

Table 2 lists some key attributes of these temperature-time curves including maximum gas temperature (T_{max}), time when maximum temperature occurs (t_{max}), total duration of fire including the cooling phase (t_u). The maximum temperature of Fire 1, Fire 2, and Fire 3 was 1040°C, 940°C, and 840°C, respectively, when the time reached about 30 min, 60 min, 120 min, respectively. The total duration of these three fires was 90 min, 165 min, and 420 min, respectively.

2.4 Temperature of steel and concrete members

A uniform temperature distribution as a function of time was assumed for the compartment fires. Four-side and three-side fire exposures were assumed for the heated columns and beams, respectively. The International Building Code (2012) requires that the structural components of buildings have at least one-hour fire-resistance rating (FRR). In this study, the Carboline Type-5MD Spay-applied fire resistive materials (SFRM) was used on the steel columns and beams to provide a one-hour FRR. The SFRM thickness required for the W14×90 column is 6 mm, and that required for the W14×22 and

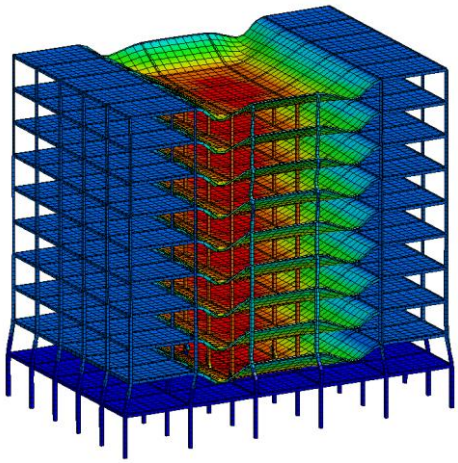

Fig. 4 Collapse mode of the gravity frame under Fire 2 and Fire 3

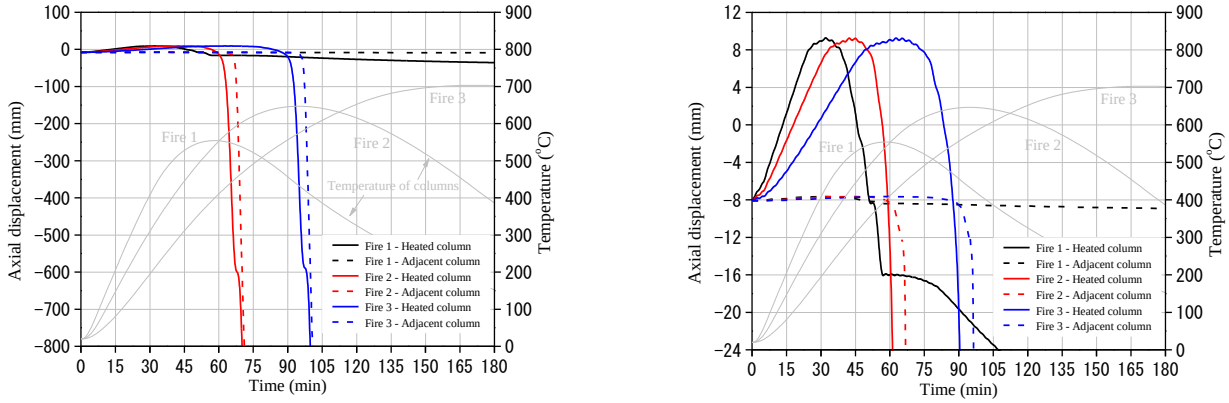

Fig. 5 Axial displacements of steel columns in different fires: (a) whole period and (b) details of the early deformation

W16×26 beams is 9 mm. The protection thickness of columns and beams was calculated according to the limiting temperature of 550 °C and 600 °C after one-hour heating, respectively. The slab was assumed to be unprotected since the temperature of reinforcement was less than its limiting temperature of 600 °C after one-hour's heating for a given concrete cover of 30 mm.

Heat transfer analyses were conducted in LS-DYNA to obtain the temperature histories of the protected structural members (beam, column, slab) which were modelled by a layered composite shell formulation. The details of the thermal model can be found in a NIST technic note (Jiang et al. 2017). The thermal and mechanical properties of this SFRM were experimentally determined by Kodur and Shakya (2013). The thermal properties of steel and concrete refer to CEN (2004, 2005). The predicted temperature-time curves of the structural members for the three fires are shown in Fig. 3. In general, the maximum temperature of structural members occurred during the cooling phase, which was delayed by at least 30 min compared to the maximum temperature of the fire curve. The delay in the steel members is due to the presence of fire protection, and the delay in the reinforcement is due to the presence of concrete cover. The steel members and concrete slabs had a similar delay period, which was about 30 min for Fire 1 and Fire 2, and 40 min for Fire 3.

In the numerical model, the temperatures of columns, beams, slabs under Fire 1, Fire 2, and Fire 3 in Fig. 3 were input. For the temperature increasing duration of these structural members, a real time of one hour was scaled down to 8 s. This means that the real heating duration of 60 min, 90 min, 180 min for members under the three fires was scaled to 8 s, 12 s, 16 s, respectively. For the temperature decreasing duration of structural members, a greater time scale was used in this study since quasi-static behavior is always obtained. The real cooling duration of 180 min, 150 min, 240 min for the three fires was scaled to 10 s, 10 s, 15 s, respectively. Therefore, the total temperature variation duration of 240 min, 240 min, 420 min for the members under the three fires was scaled down to a total simulation time of 18 s, 22 s, 31 s, respectively.

3 Collapse behavior of protected gravity frames u nder compartment fires

The behavior of gravity frames (Fig. 1) exposed to

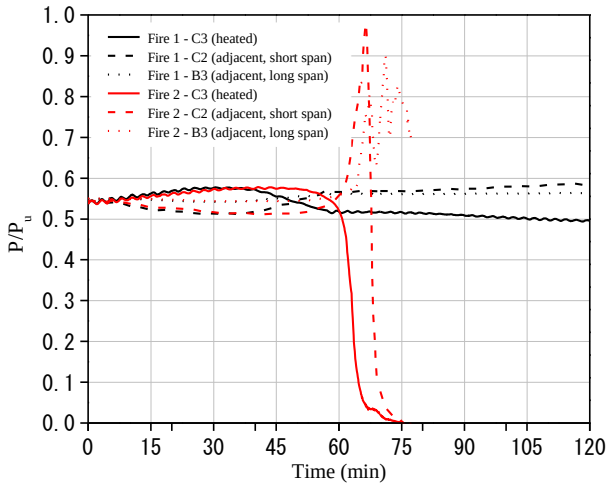

Fig. 6 Axial forces in the steel columns for different fires

compartment fires with a cooling phase (Fig. 2) was first investigated. The frame withstood Fire 1, but collapsed under Fire 2 and Fire 3, as shown in Fig. 4. The collapse was triggered by the buckling of the heated columns (C3, C4, D3, D4) in the fire compartment, followed by the buckling of the adjacent columns (C2, C5, D2, D5) along the short span. Afterwards, the surrounding frame moved laterally towards the fire compartment driven by the large deflection of beams and slabs. The variation of axial displacements of the heated columns and adjacent cool columns under the three fires is shown in Fig. 5. The temperature of the heated column is also shown in the figure (marked in gray). For all the fires, the top of the heated columns rapidly moved upwards by about 16 mm due to the thermal expansion effect, and the upward movement slowed down when the column temperature reached 400°C, above which the yield strength of steel started to degrade at elevated temperatures as pre-defined in the material properties. This plateau of axial displacements of columns lasted about 15 min, 18 min and 25 min for Fire 1, Fire 2, and Fire 3, respectively. As the material properties continued to degrade, the heated columns buckled at 60 min and 90 min for Fire 2 and Fire 3, respectively. This time corresponded to a column temperature of about 550°C for both cases, which is equal to the pre-defined critical temperature of columns when determining its fire-resistance rating. The failure time of the heated column is defined as the time when its axial displacement returns to its initial position. After this point, there is a sudden increment in the axial displacement and reduction in the axial force. The variation of axial forces in the heated and adjacent columns is shown in Fig. 6, where P is the axial forces in the column and P_u is the ultimate capacity of the column. It shows that for a restrained column at elevated temperatures, the load ratio (P/P_u) increased slightly (from initial value of 0.54 to maximum value of 0.57) due to the restrained thermal expansion. For Fire 2, the load previously sustained by the heated columns were transferred to the surrounding columns, leading to the buckling of the adjacent column C2 along the short span when its load ratio reached 1.0.

After the buckling of the heated and adjacent columns, the heated beam lost its vertical support and the span increased to three times the initial value. Large tensile forces were generated in the beam, which drove the surrounding frame to move laterally. A maximum tensile force of about 500 kN was found at the end of the 9-m beam (connected to the column B3) adjacent to the heated beam. It is about 35% of its yielding force (F_y=1410 kN for yielding of the full section). This magnitude (500 kN) is higher than the measured tensile force of 345 kN in fire tests on unprotected steel-concrete composite floor (Wald *et al*. 2009). This indicates that the beam-to-column connection should possess a sufficient tensile capacity of one-third of the yielding capacity of the beam to prevent fracture failure during the fire. The fracture failure of connections will lead to the loss of lateral support for the connected column, which increase its effective length and thus lead to its failure in buckling.

The survival of the frame in Fire 1 is because of the early cooling down of the fire. The temperature of the heated columns reached the critical temperature of 550℃, but its temperature reduced just after it. The recovery of its strength prevented its further failure, and the frame did not collapse.

For a given design fire, the heat transfer analysis of steel members in the fire compartment is first conducted. The collapse time of the frame can be conservatively determined by the time when the temperature of steel columns reached a critical temperature of 550°C. If the column temperature is lower than 550°C, we can conclude that the frame will not collapse.

4 Mitigation of progressive collapse

The collapse mechanism of gravity frames under single-compartment fires (see Fig. 4) can be divided into three stages: (1) buckling of the heated columns in the fire compartment; (2) buckling of the adjacent columns at ambient temperature; (3) lateral drift of surrounding frame. Strategies to mitigate collapse can be proposed based on these three collapse stages. Firstly, the buckling of the heated columns can be prevented by increasing the fire protection level. For a standard fire with

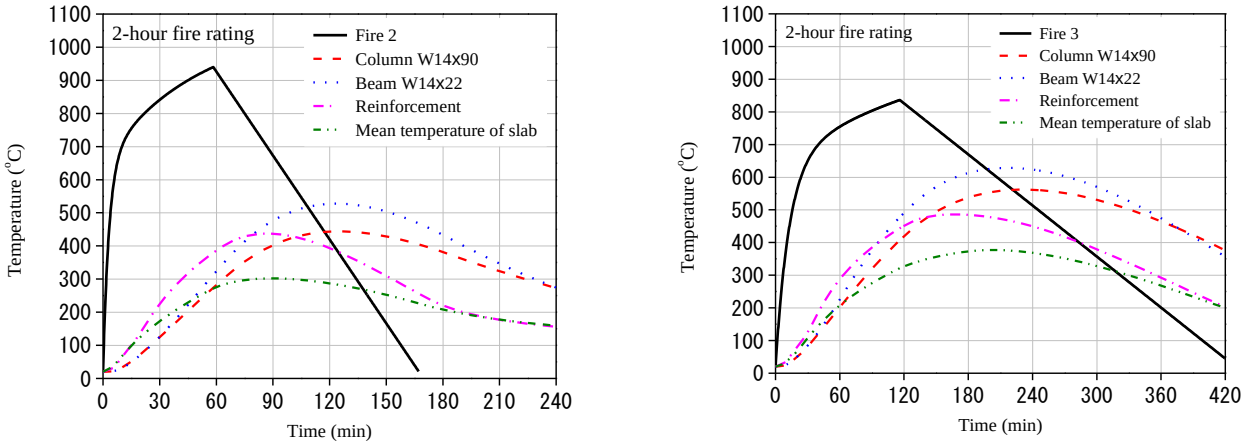

Fig. 7 Temperature-time curves of steel and concrete members for 2-hour fire-resistance rating: (a) Fire 2 and (b) Fire 3

a heating phase alone, the enhanced fire-resistance rating can only delay the failure of a heated column, rather than preventing its failure. However, for a realistic fire with a cooling phase, a higher fire-resistance rating may lead to a lower temperature in a structural member than its critical temperature; Secondly, the buckling of the adjacent columns is due to the uneven load redistribution in the plan direction. A more uniform load redistribution to the columns far away from the heated columns can be used to prevent the failure of the adjacent columns. This can be achieved by adding hat braces (or hat truss system) on the top floor of the frame to uniformly redistribute the loads previously sustained by the buckled columns; Thirdly, the lateral drift of the surrounding frame can be mitigated by using vertical braces along the height of the frame. In the following subsections, the feasibility of using these methods on mitigating the collapse of gravity frames was investigated.

4.1 Enhancement of fire protection levels

In this section, a higher fire-resistance rating of two hours was assumed for the structural members. This corresponds to a fire protection thickness of 14 mm and 18 mm for the steel columns and beams, respectively. It was assumed that the slab had the same temperature distribution as the one-hour rating case. The temperature-time curves of steel and concrete members are shown in Fig. 7. The frame did not collapse in Fire 2 since the maximum temperature of the columns was only about 450℃, which was lower than its critical temperature of 550℃. While the frame collapsed at 190 min in Fire 3. Note that the occurrence of collapse was during the cooling phase. This is because the presence of a thicker SFRM significantly delayed the temperature increment of steel columns. For a lower level of fire protection such as one-hour FRR, Fire 2 is severer than Fire 3 since the frame collapsed at 60 min in Fire 2 compared to 90 min in Fire 3 (Fig. 5). However, for a higher level of fire protection such as two-hour FRR, Fire 3 became severer than Fire 2 since the frame collapsed in Fire 3 but survived in Fire 2. This indicates that the severity of fires depends on the fire protection level on the structural members. It is suggested to consider the potential fire scenario when determine the fire-resistance rating in addition to the importance of the building. For example, as specified in Table 601 of International Building Code (2012), the B group of Type-I buildings requires a fire-resistance rating of 2 hours. If a "long-cool" fire similar to Fire 3 is chosen for the design fire, it is suggested to increase the fire rating level to 3 hours since the building may collapse as found in this study.

4.2 Use of horizontal bracing systems

Increasing the fire protection level alone cannot effectively guarantee the stability of buildings since the protected heated columns can still buckle as long as the fire fuel is sufficient. To facilitate a uniform redistribution of loads after the buckling of the heated columns becomes an alternative. In this study, a horizontal bracing system arranged on the top floor of buildings (i.e., hat bracing or roof truss) was used to achieve a more uniform load redistribution pattern. Two arrangements of hat braces were considered: hat braces along perimeter alone (Hat-perimeter) and hat braces on the whole floor (Hat-wholeFloor). The layout of Hat-perimeter is shown in Fig. 8, and internal braces are included between columns for Hat-wholeFloor. Inverted V-bracing systems, commonly applied in concentrically braced frames (CBF), were used in this study. The braces along the long and short span had a length of 6 m and 5 m, respectively. A square hollow structural section (HSS) of 152×152×10 and 140×140×10 was used for the 6-m and 5-m braces, respectively. The dimension was determined for special concentrically braced frames (SCBF) according to AISC 341 (2005). The fire scenario of Fire 2 on Floor 2 was used in the following sections.

Fig. 9 shows a comparison of behavior of the frames in Fire 2, where the frame with Hat-perimeter collapsed but that with Hat-wholeFloor withstood the fire. The roof was removed in the figure to show the deformation of braces. It was found that the perimeter arrangement of hat braces had little effect on the buckling of the heated and adjacent columns, and also on the load redistribution among the internal columns. The braces along the long span buckled due to the significant lateral drift of the frame after the

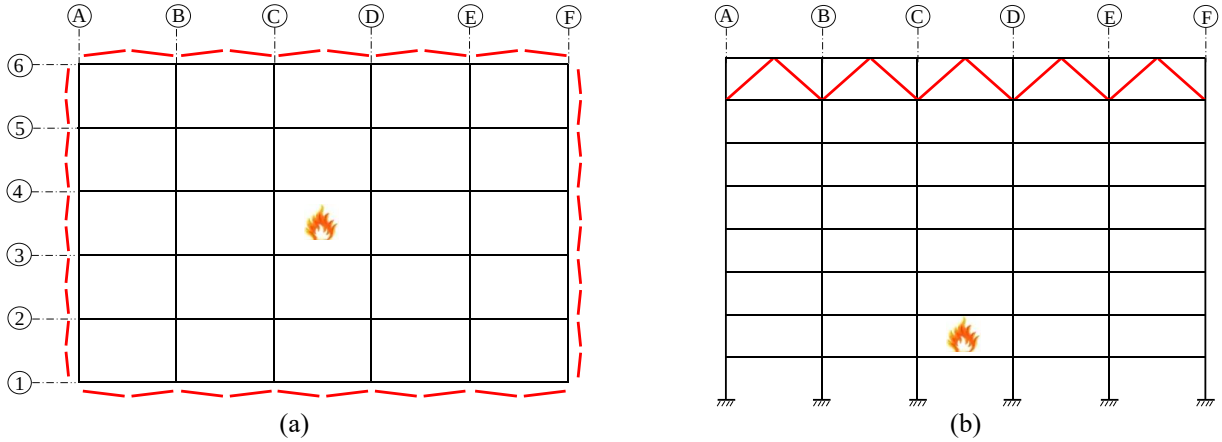

(a) (b)

Fig. 8 Layout of horizontal bracing system at perimeter of the top floor (Hat-perimeter): (a) plan view and (b) elevation view

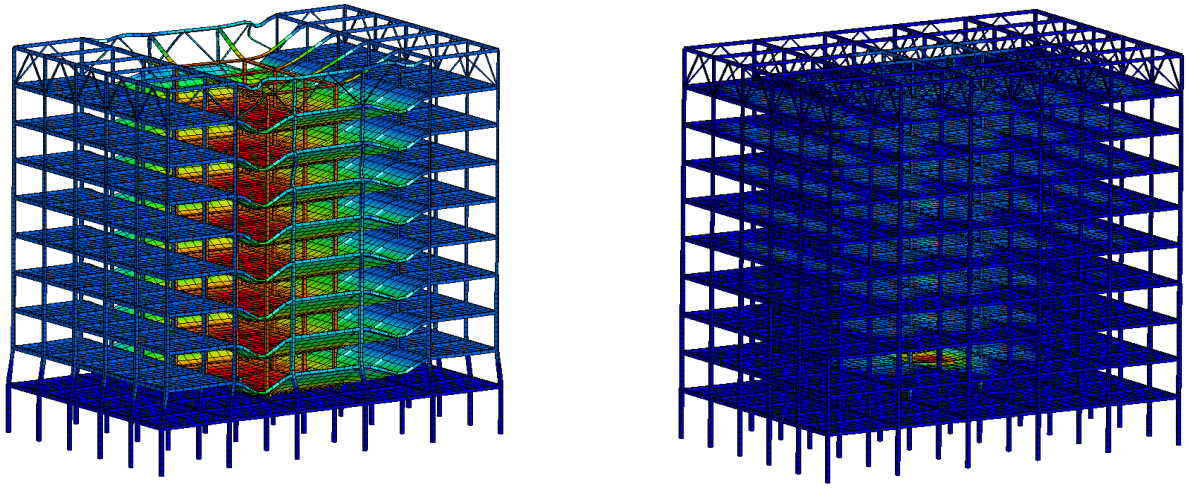

(a) (b)

Fig. 9 Behavior of the frame in Fire 2 with: (a) Hat-perimeter (collapse) and (b) Hat-wholeFloor (withstand)

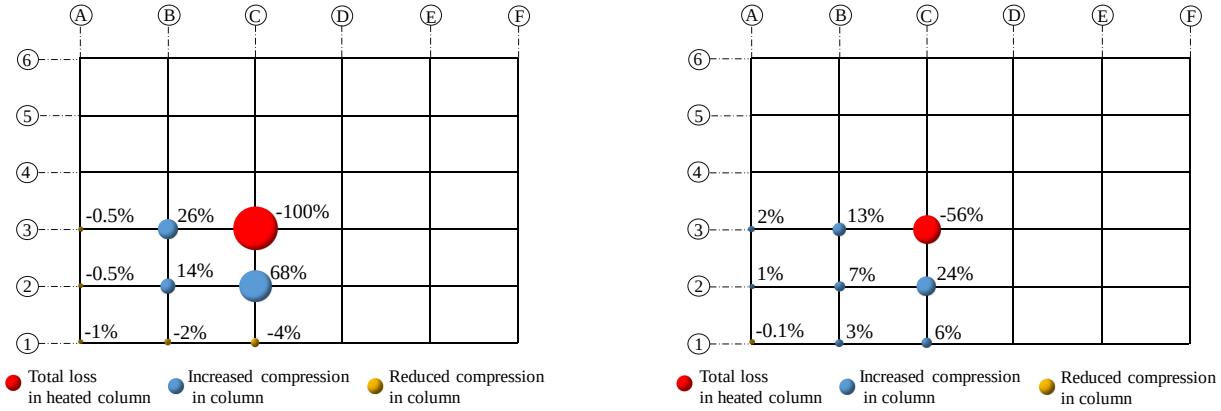

(a) (b)

Fig. 10 Load redistribution in adjacent columns in the frame under Fire 2: (a) unbraced; (b) Hat-wholeFloor

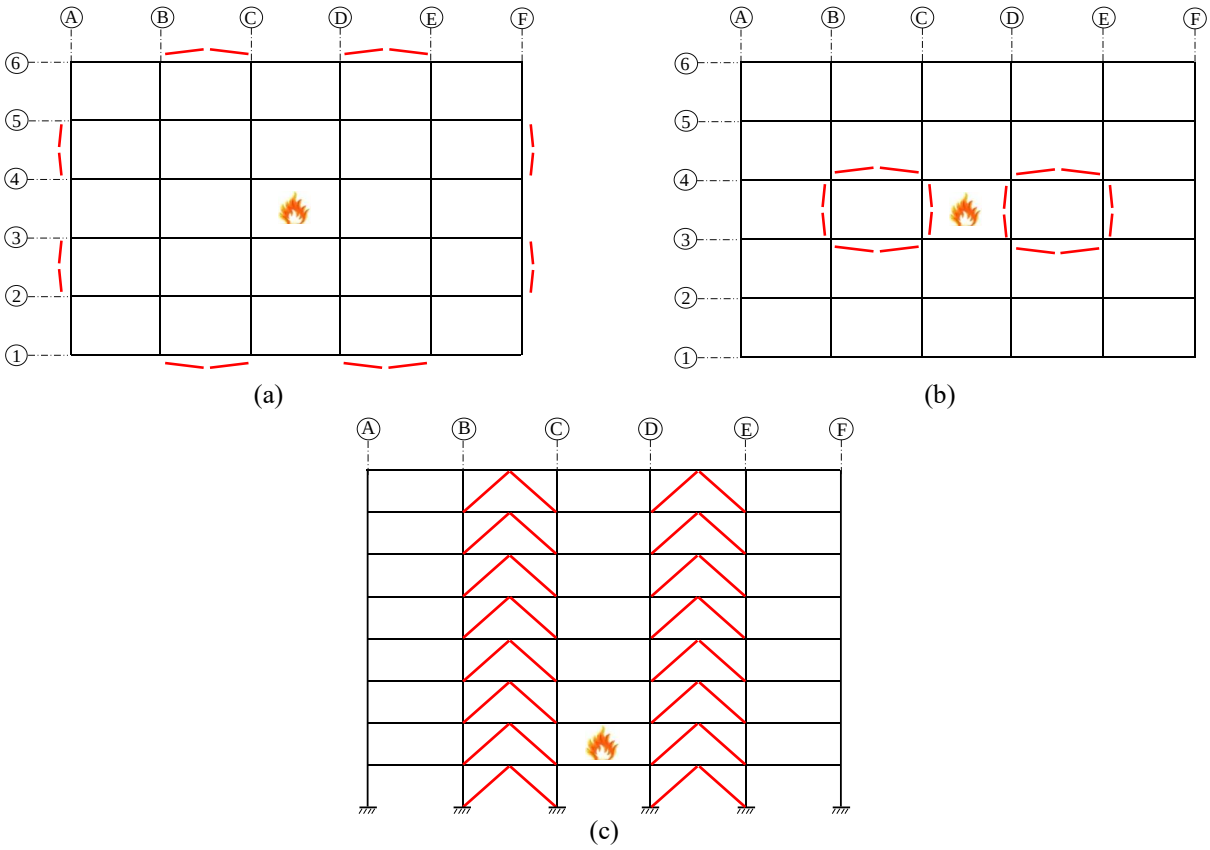

Fig. 11 Layout of vertical bracing system: (a) plan view of Vertical-perimeter, (b) plan veiw of Vertical-internal and (c) elevation view

buckling of the adjacent columns. For the frame with hat braces on the whole floor (Hat-wholeFloor), no buckling of braces occurred and the brace uniformly redistributed the load to the surrounding columns. Fig. 10 shows a comparison of percentage of load redistribution to all the columns on the fire compartment floor of the frames with and without Hat-wholeFloor. The percentage of redistributed loads on each column was calculated as the ratio of the change of axial forces in it to the initial load applied on the heated column (column C3 in this case), i.e., $\Delta P/P_0$(C3). The positive and negative values represented the increment and decrement in the compression of the columns. The ball in red represents the heated column C3. The balls in yellow represent the columns with reduced compressive forces (negative) and the blue ones denote those with increased compressive forces (positive). The heated column in the unbraced frame lost its strength after buckling, while the heated column in the frame with Hat-wholeFloor had a residual strength of about 44 % of its initial compression force. This means that the hat bracing system reduced the total amount of redistributed load. The hat bracing also lead to a more uniform load redistribution form. As shown in Fig. 10, more loads were transferred to the columns along the short span. For this reason, the column C2 first buckled after the buckling of the heated column C3 (Fig. 6). The ratio of load redistribution along the short and long span is almost 2.6:1 and 1.8:1 for the frame with and without hat bracing, respectively. The hat bracing redistributed the load to the columns at perimeter (increased compression), compared to a reduced compression in the perimeter columns in theframe without the braces which was pulled out by the large deflection.

The effectiveness of horizontal bracing systems may depend on the location of fires. Under a corner fire, the frame with a Hat-perimeter bracing system did not collapse due to the contribution of braces just above the fire compartment to load redistribution in adjacent columns. The presence of horizontal braces in the middle height of the frame (belt bracing) had a significant effect on the collapse resistance. Therefore, it is recommended to arrange a combined hat and belt bracing systems in view of the uncertainty of fire locations.

4.3 Use of vertical bracing systems

A vertical bracing system placed along the entire height of the building was used in this section. Two plan layouts of the bracing systems were accounted for: braces arranged in two edge bays along the perimeter of the frame (i.e., Vertical-perimeter as shown in Fig. 11(a)) and braces placed in the internal bays of the frame (i.e., Vertical-internal as shown in Fig. 11(b)). The second bracing system is representative of lift shaft placed in the interior of a building. A square HSS was used for the braces, and its dimension was determined for special concentrically braced frames (SCBF) according to

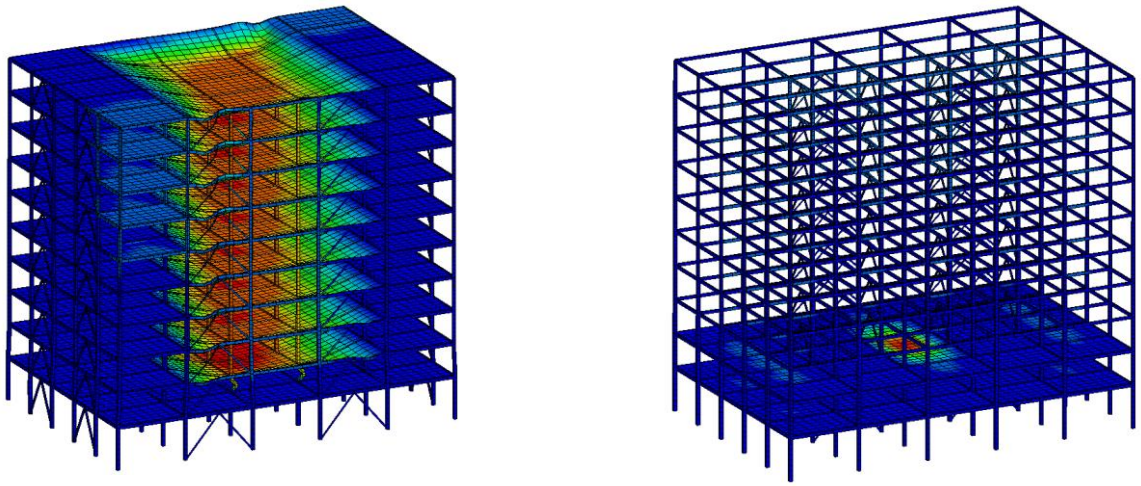

(a) (b)

Fig. 12 Behavior of the frame in Fire 2 with: (a) Vertical-perimeter (withstand); (b) Vertical-internal (withstand)

Table 3 Design of vertical braces along the height of the frame

Floor level	6-m braces along the long span	5-m braces along the short span
1-2	HSS 203×203×13	HSS 178×178×13
3-7	HSS 178×178×13	HSS 152×152×13
7-10	HSS 152×152×10	HSS 140×140×10

Table 4 Summary of behavior of frames in realistic fire

Case No.	Fire	Bracing type	FRR	Collapse or not	Collapse time (min)	F_{max} (beam) (kN)	δ_{max} (slab) (mm)
1	Fire 1	Unbraced	1-h	No	/	1410	55
2	Fire 2	Unbraced	1-h	Yes	60	500	590
3	Fire 3	Unbraced	1-h	Yes	90	500	570
4	Fire 2	Unbraced	2-h	No	/	1110	565
5	Fire 3	Unbraced	2-h	Yes	190	480	627
6	Fire 2	Hat-perimeter	1-h	Yes	60	500	590
7	Fire 2	Hat-wholeFloor	1-h	No	/	1350	610
8	Fire 2	Vertical-perimeter	1-h	No	/	1310	600
9	Fire 2	Vertical-internal	1-h	No	/	1400	540

Note: FRR=fire-resistance rating; F_{max} (beam)=maximum tensile force in steel beam; δ_{max} (slab)=maximum deflection of slab

AISC 341 (2005). The dimensions of 6-m and 5-m braces used for various stories are shown in Tables 3.

The frames with vertical bracing systems withstood the fire, as shown in Fig. 12. For the frame with Vertical-perimeter, the heated and adjacent columns buckled, but the lateral drift of surrounding frame was mitigated by the vertical braces. The floors experienced large deflection, but the building did not globally collapse. However, this large deflection of slabs is somewhat unaccepted because the building cannot be used after the fire although it survives in the fire. In contrast, no columns buckled in the frame with Vertical-internal as the braced bay is just adjacent to the fire compartment. The large deflection was resisted by the bracing system.

5 Summary and discussion

In this study, the collapse behavior of 9 frames with different fire curves, fire-resistance ratings, bracing systems was investigated, as summarized in Table 4. It was found that Fire 3, a "long-cool" fire, is the severest fire since the unbraced frame with 2-h fire-resistance rating collapsed at 190 min. The collapse time is 70-min delayed compared to the two-hour rating, due to the cooling phase. The application of hat or vertical bracing systems can effectively mitigate or prevent the collapse of the frame. For the collapsed frame (Cases 2, 3, 5, 6), the tensile force in the steel beam reached a maximum value of about 500 kN, which occurred at the end of the 9-m beam adjacent to heated beam. For the

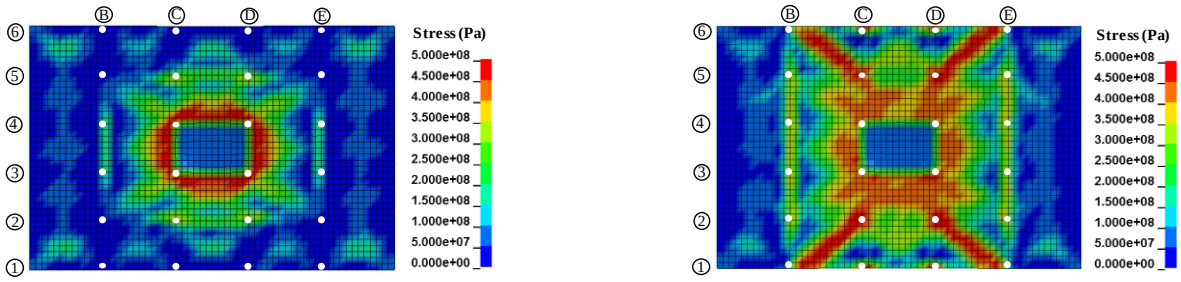

(a) (b)

Fig. 13 Distribution of maximum in-plane stress in the reinforcement of the slabs: (a) large deflection of slabs in a limited region and (b) larger deflection of slabs in a wider region

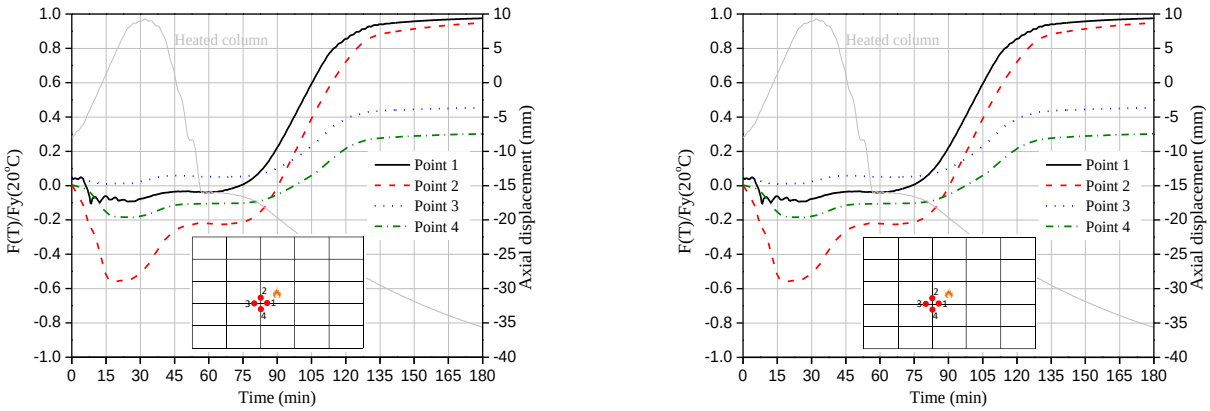

(a) (b)

Fig. 14 Variation of axial forces in connections of the frame under: (a) Fire 1 and (b) Fire 2

withstanding frame (Cases 1, 4, 7, 8, 9), significantly higher tensile forces were found at the end of the heated beam when it cooled down to ambient temperature. These maximum tensile forces in the steel beam varies in a range of 80 %-100 % of its yielding force at ambient temperature (F_y=1410 kN when the whole section yield). This means that the beam-to-column connections should be designed to resist high tensile forces during the cooling phase of a fire, up to a level of the yielding force of beams. For all the cases except Case 1, the slab experienced large deflection without collapse. The maximum deflection of slabs reached a level of about *span*/10 (600 mm in this case), which is double the generally accepted deformation limit of *span*/20. This means the slab may resist loads at a larger deflection through tensile membrane action.

After the failure of the heated columns, the connection and beam above the failed column may experience large axial forces. This axial force will be transferred to the adjacent connections through catenary action of the beam. The load previously sustained by the failed column is transferred to the adjacent beams and columns by slabs. The deflection of slabs has a great impact on the horizontal displacement at the top of columns, thus influencing their stability through P-Δ effect. The effect of slabs and connections on the collapse resistance of structures is discussed in the following subsections, and recommendations for the selection of bracing systems and design fire scenarios are also presented.

5.1 Effect of slabs

As temperature increases, the deflection of the heated slab in the fire compartment increases and its load bearing mechanism may change from bending to tensile membrane action. At the early stage of fire, the buckling of columns is confined in the fire compartment, the tensile forces in the reinforcement of the heated slab are resisted by a tensile ring around its perimeter provided by the reinforcement of adjacent slabs at ambient temperatures, as shown in Fig. 13(a) (the white points represent columns). As the buckling of columns spreads to a larger range, the tensile forces in the reinforcement of slabs are also resisted by four tensile yielding lines extended to the edge of the frame, as shown in Fig. 13(b). The load bearing mechanism of slabs is important for the collapse resistance of frames since greater deflections of the slab will lead to greater lateral displacements of columns, and thus a greater P-Δ effect and lower stability. It is suggested to increase the cross-section of columns along the edges of the frame to provide strong resistance for the development of tensile forces in the reinforcement of slabs.

5.2 Effect of connections

The axial forces in the heated and ambient connections for Fire 1 and Fire 2 were presented in Fig. 14. For Fire 1,

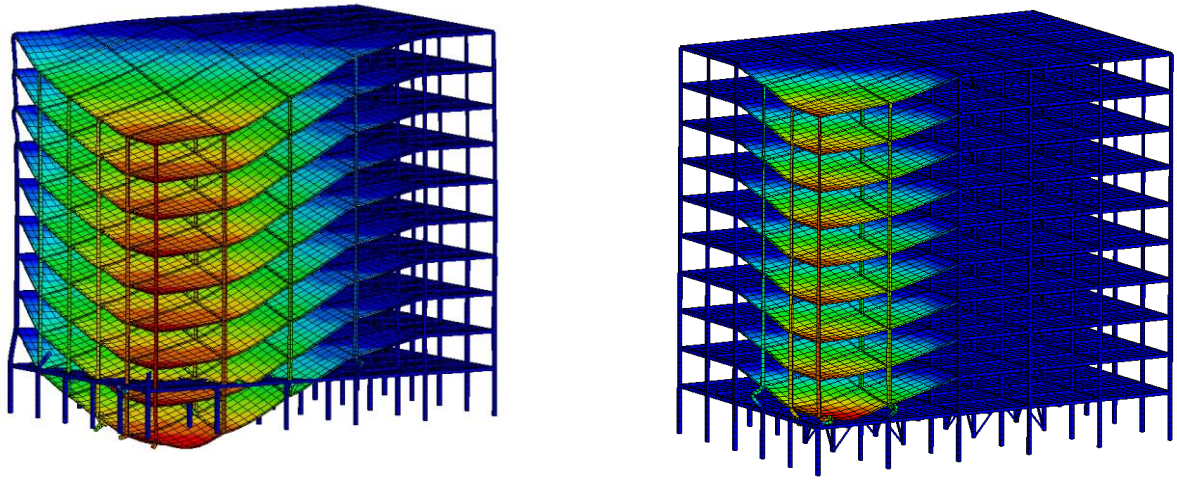

(a) (b)

Fig. 15 Behavior of the frame in Fire 2 at the corner with: (a) unbraced (complete collapse) and (b) Vertical-internal (partial collapse)

as temperatures increased, there were large compression forces in the heated connections (Point 1 and 2) due to the restrained thermal expansion. The connection along the short span (Point 2) had a much greater compression force than that along the long span (Point 1) due to the greater axial restraint in that direction. After the column temperature started to decrease at 60 min, the connections subjected to large tensile forces in the cooling phase as the deflection of the heated column increased. The magnitude of tensile forces in the connection reached a level of its yield force. In this case, the failed column had a residual strength due to the recovery of material properties just after its failure. This residual strength provided certain vertical support for the slab, and thus the deflection of the slab was limited and no significant tensile membrane action was formed. A different variation of axial forces in the connections was found for Fire 2 where the frame collapsed. The heated columns completely failed, and the slab experienced large deflections where tensile membrane action contributed more to the load bearing capacity of the frame. The tensile forces in the beams and connections were limited. Therefore, the impact of connections on the collapse resistance of structures depends on the temperature time history, residual strength of columns, deflection of slabs. More attention should be paid to prevent fracture of connections during the cooling phase, and also to large compression force in the connections during the heating phase. Further work is needed to investigate the impact of different types of connections on progressive collapse of steel structures.

5.3 Recommendations for selecting bracing systems

It was found in this study that use of a single type of bracing systems (horizontal or vertical) is sufficient to prevent the collapse of frames under an internal single-compartment fire. A corner fire on Floor 2 (Fire 2 within grid line A, B, 1, 2) was also considered in this study, and the behavior of unbraced and braced frames under this corner fire is shown in Fig. 15. The unbraced frame globally collapsed (Fig. 13(a)), while the frame with Vertical-internal partially collapsed (the fire compartment and upper floors collapsed). The braced frames with Hat-wholeFloor or Vertical-perimeter withstood the fire (not shown in the figure) where no buckling of columns occurred. Although the presence of internally-arranged vertical braces did not prevent the collapse of the fire compartment, it acted as a barrier to prevent the spread of collapse to the remaining part of the frame. By comparing Fig. 15(b) and Fig. 12(a), it was found that local collapse of a frame may occur if the vertical bracing system was placed at perimeter or interior, but the global collapse will be prevented. It is therefore recommended to use a combination of perimeter and internal vertical bracing systems to prevent local collapse. Using hat bracing system on the whole top floor is the best measure to prevent progressive collapse, since it can not only uniformly redistribute the load but reduce the deflection of slabs. For high-rise buildings, there are always several strengthened stories along the height of the building where belt trusses are arranged at the perimeter. It is recommended to also arrange outrigger truss and radial truss system at the interior of the strengthened story.

5.4 Recommendations for selecting fire scenarios

A key step for performance-based fire safety design is to establish a list of fire scenarios, represented by fire locations, building characteristics, occupant responses, fire loads, fire protection systems. The fire location is determined through a combination of most-likely and worst-case assumptions, and thus each fire scenario has either a high probability of occurrence, serious consequences or both. The main challenge in scenario selection is to find a manageable number of fire scenarios that are sufficiently diverse and representative, and therefore if the design is safe for those scenarios, then it should be safe for all scenarios. Based on the results in this study, it is recommended to pay more attention to “long-cool” fires which always last for a longer time with a relatively

lower maximum temperature. This is because the protected structural members will have higher temperatures compared to mild fires due to its longer period of heating.

6 Conclusions

This paper investigated the collapse behavior of three-dimensional steel-framed gravity buildings subjected to realistic fires with a cooling phase. The effect of fire protections and bracing systems on the collapse resistance was studied. The following conclusions can be drawn:

- Whether a gravity building collapses or not in a realistic fire significantly depends on the duration of its heating phase. The building can withstand a "short-hot" fire, but collapse under a mild fire and "long-cool" fires. The survival of the building in a short-hot fire is due to the early cooling down of gas temperatures, leading to reduced temperature of the heated columns after reaching its critical temperature.
- Gravity buildings may collapse during the heating phase or the cooling phase of a fire. The collapse time can be conservatively determined by the time when the temperature of steel columns reaches a critical temperature of 550°C.
- The collapse of gravity buildings is typically triggered by the buckling of the heated columns in the fire compartment, followed by the buckling of the adjacent columns along the short span. This is further followed by obvious lateral drift of the surrounding frame driven by the large deflection of beams and slabs.
- The severity of real fires with a cooling phase depends on the fire protection level on the structural members. A higher level of fire protection may prevent the collapse of structures, but may also lead to collapse in the cooling phase due to the delayed increment of temperatures in the heated members.
- The tensile membrane action in a heated slab can be resisted by a tensile ring around its perimeter provided by the reinforcement of adjacent slabs at ambient temperature or by tensile yielding lines extended to the edge of the frame. The maximum deflection of slabs may reach a level of about *span*/10. It is suggested to strengthen the columns along the edges of the frame to facilitate formation of tensile membrane action in slabs.
- It is suggested that the beam-to-column connections should be designed to resist high tensile forces during the cooling phase of a fire, up to a level of the yielding force of beams.

It is recommended to consider the potential fire scenario when determine the fire-resistance rating in addition to the importance of buildings. It was found that a "long-cool" fire was more dangerous, and it is suggested to increase the fire-resistance rating determined according to the importance of a structure to prevent its collapse under a "long-cool" fire. The application of hat or vertical bracing systems can effectively mitigate or prevent the collapse of gravity buildings. It is recommended to arrange hat bracing systems on the whole top floor of a building, while to use a combination of perimeter and internal vertical bracing systems. These findings are applicable to single-compartment fires in this study, and further work is needed to consider severer fire scenarios such as multi-compartment fire and travelling fire.

Acknowledgements

The work presented in this paper was supported by the National Natural Science Foundation of China with grant 51538002.

References

AISC (American Institute of Steel Construction). (2005), "Seismic Provisions for Structural Steel Buildings." *AISC 341*, Chicago.

Alashker, Y., EI-Tawil, S. and Sadek, F. (2010), "Progressive collapse resistance of steel-concrete composite floors", *J. Struct. Eng.*, **136** (10), 1187-1196. https://doi.org/10.1061/(ASCE)ST.1943-541X.0000230.

Ali, H.M., Senseny, P.E. and Alpert, R.L. (2004), "Lateral displacement and collapse of single-storey steel frames in uncontrolled fires", *Eng. Struct.*, **26**, 593-607. https://doi.org/10.1016/j.engstruct.2003.12.007.

ASCE (American Society of Civil Engineers). (2005), "Minimum Design Loads for Buildings and Other Structures", *ASCE 7*, Reston, Virginia.

CEN (European Committee for Standardization). (2002), "Actions on structures, Part 1.2: General Actions – Actions on Structures Exposed to Fire", EN 1991-1-2, Brussels.

CEN (European Committee for Standardization). (2004), "Design of concrete structures, Part 1.2: General Rules - Structural Fire Design", EN 1992-1-2, Brussels.

CEN (European Committee for Standardization). (2005), "Design of steel structures, Part 1.2: General Rules-Structural Fire Design", EN 1993-1-2, Brussels.

Cesarek, P., Kramar, M. and Kolsek, J. (2018), "Effect of creep on behaviour of steel structural assemblies in fires", *Steel Compos. Struct.*, **29**(4), 423-435. https://doi.org/10.12989/scs.2018.29.4.423.

Cowlard, A., Bittern, A., Abecassis-Empis, C. and Torero, J. (2013), "Fire safety design for tall buildings", *Proceedings of the 9th Asia-Oceania Symposium on Fire Science and Technology*, Procedia Engineering, **62**, 169-181. https://doi.org/10.1016/j.proeng.2013.08.053.

DoD (Department of Defense). (2010), "Design of Buildings to Resist Progressive Collapse", *UFC 4-023-03*, Washington, DC.

Davoodnabi, S.M., Mirhosseini, S.M. and Shariati, M. (2019), "Behavior of steel-concrete composite beam using angle shear connectors at fire condition", *Steel Compos. Struct.*, **30**(2), 141-147. https://doi.org/10.12989/scs.2019.30.2.141.

Fang, C., Izzuddin, B.A., Obiala, R., Elghazouli, A.Y. and Nethercot, D.A. (2012), "Robustness of multi-storey car parks under vehicle fire", *J. Constr. Steel. Res.*, **75**, 72-84. https://doi.org/10.1016/j.jcsr.2012.03.004.

Ferraioli, M. (2019), "Evaluation of dynamic increase factor in progressive collapse analysis of steel frame structures considering catenary action", *Steel Compos. Struct.*, **30**(3), 253-269. https://doi.org/10.12989/scs.2019.30.3.253.

Flint, G., Usmani, A.S., Lamont, S., Lane, B. and Torero, J. (2007), "Structural response of tall buildings to multiple floor fires", *J. Struct. Eng.*, **133**(12), 1719-1732. https://doi.org/10.1061/(ASCE)0733-9445(2007)133:12(1719).

GSA (General Services Administration). (2003), "Progressive Collapse Analysis and Design Guidelines for New Federal

Office Buildings and Major Modernization Projects", Washington, DC.

Huang, Y., Wu, Y. and Chen, C.H. (2019), "Dynamic increase factor for progressive collapse of semi-rigid steel frames with extended endplate connection", *Steel Compos. Struct*., **31**(6), 617-628. https://doi.org/10.12989/scs.2019.31.6.617.

Huang, Z., Burgess, I.W. and Plank, R.J. (2000), "Effective stiffness modelling of composite concrete slabs in fire", *Eng. Struct.*, **22**(9), 1133-1144. https://doi.org/10.1016/S0141-0296(99)00062-0.

Hughes, T.J.R. and Liu, W.K. (1981), "Nonlinear Finite Element Analysis of Shells: Part I. Three-Dimensional Shells", *Comp. Meth. Appl. Mech.*, **27**, 331-362. https://doi.org/10.1016/0045-7825(81)90121-3.

IBC (International Building Code). (2012). International Code Council, IL, USA.

Izzuddin, B.A., Tao, X.Y. and Elghazouli, A.Y. (2004), "Realistic modelling of composite and R/C floor slabs under extreme loading-Part I: Analytical method", *J. Struct. Eng.*, **130**(12), 1972-1984. https://doi.org/10.1061/(ASCE)0733-9445(2004)130:12(1972).

Jiang, B.H., Li, G.Q. and Izzuddina, B.A. (2016), "Dynamic performance of axially and rotationally restrained steel columns under fire", *J. Constr. Steel. Res.*, **122**, 308-315. https://doi.org/10.1016/j.jcsr.2016.03.013.

Jiang, B.H., Li, G.Q., Li, L.L. and Izzuddin, B.A. (2018), "Experimental studies on progressive collapse resistance of steel moment frames under localized furnace loading", *J. Struct. Eng.*, **144**(2), 04017190. https://doi.org/10.1061/(ASCE)ST.1943-541X.0001947.

Jiang, J. and Li, G.Q. (2017a), "Progressive collapse analysis of 3D steel frames with concrete slabs exposed to localized fire", *Eng. Struct.*, **149**, 21-34. https://doi.org/10.1016/j.engstruct.2016.07.041.

Jiang, J. and Li, G.Q. (2017b), "Disproportional collapse of 3D steel-framed structures exposed to various compartment fires", *J. Constr. Steel. Res.*, **138**, 594-607. https://doi.org/10.1016/j.jcsr.2017.08.007.

Jiang, J., Main, J.A., Sadek, F. and Weigand, J. (2017), "Numerical modeling and analysis of heat transfer in composite slabs with profiled steel decking", NIST Technical Note 1958, National Institute of Standards and Technology, Gaithersburg, MD. https://doi.org/10.6028/NIST.TN.1958.

Jiang, J. and Li, G.Q. (2018), "Progressive collapse of steel high-rise buildings exposed to fire: Current state of research", *Int. J. High-rise Build.*, **7**(4), 375-387. https://doi.org/10.21022/IJHRB.2018.7.4.375.

Jiang, J., Main, J.A., Weigand, J. and Sadek, F. (2020), "Reduced-order modeling of composite floor slabs in fire. II: Thermal-structural analysis", *J. Struct. Eng.*, **146**(6), 04020081. https://doi.org/10.1061/(ASCE)ST.1943-541X.0002607.

Kim, J. and Park, J.. (2008), "Design of steel moment frames considering progressive collapse", *Steel Compos. Struct.*, **8**(1), 85-98. https://doi.org/10.12989/scs.2008.8.1.085.

Kirby, B.R. (1997), "British steel technical European fire test program design, construction and results. Fire, static and dynamic tests of building structures." London.

Kodur, V.K.R. and Shakya, A.M. (2013), "Effect of temperature on thermal properties of spray applied fire resistive materials", *Fire Saf. J.*, **61**, 314-323. https://doi.org/10.1016/j.firesaf.2013.09.011.

Lim, O.K., *et al*. (2019), "Experimental studies on the behaviour of headed shear studs for composite beams in fire", *Steel Compos. Struct.*, **32**(6), 743-752. https://doi.org/10.12989/scs.2019.32.6.743.

Lien, K.H., Chiou, Y.J., Wang, R.Z. and Hsiao, P.A. (2009), "Nonlinear behavior of steel structures considering the cooling phase of a fire", *J. Constr. Steel. Res.*, **65**, 1776-1786. https://doi.org/10.1016/j.jcsr.2009.03.015.

Ma, K.Y. and Richard Liew, J.Y. (2004), "Nonlinear plastic hinge analysis of three-dimensional steel frames in fire", *J. Struct. Eng.*, **130**(7), 981-990. https://doi.org/10.1061/(ASCE)0733-9445(2004)130:7(981).

Main, J.A. and Sadek F. (2012), "Robustness of steel gravity frame systems with single-plate shear connections", NIST Technical Note 1749, National Institute of Standards and Technology, Gaithersburg, MD. https://doi.org/10.6028/NIST.TN.1749.

Menchel, K., Massart, T., Rammer, Y. and Bouillard, P. (2009), "Comparison and study of different progressive collapse simulation techniques for RC structures", *J. Struct. Eng.*, **135**(6), 685-697. https://doi.org/10.1061/(ASCE)0733-9445(2009)135:6(685).

Mirtaheri, M. and Zoghi, M.A. (2016), "Design guides to resist progressive collapse for steel structures", *Steel Compos. Struct.*, **20**(2), 357-378. https://doi.org/10.12989/scs.2016.20.2.357.

Pantousa, D. and Mistakidis, E. (2017), "Rotational capacity of pre-damaged I-section steel beams at elevated temperatures", *Steel Compos. Struct.*, **23**(1), 53-66. https://doi.org/10.12989/scs.2017.23.1.053.

Pham, X.D. and Tan, K.H. (2013), "Membrane actions of RC slabs in mitigating progressive collapse of building structures", *Eng. Struct.*, **55**, 107-115. https://doi.org/10.1016/j.engstruct.2011.08.039.

Porcari, G.L.F, Zalok, E. and Mekky, W. (2015), "Fire induced progressive collapse of steel building structures: A review of the mechanisms", *Eng. Struct.*, **82**, 261-267. https://doi.org/10.1016/j.engstruct.2014.09.011.

Rezvani, F.H., Jeffers, A.E. and Asgarian, B. (2017), "Effect of column loss location on structural response of a generic steel moment resisting frame", *Steel Compos. Struct.*, **25**(2), 217-229. https://doi.org/10.12989/scs.2017.25.2.217.

Richard Liew, J.Y. and Chen, H. (2004), "Explosion and fire analysis of steel frames using fiber element approach", *J. Struct. Eng.*, **130**(7), 991-1000. https://doi.org/10.1061/(ASCE)0733-9445(2004)130:7(991).

Sadek, F., El-Tawil, S. and Lew, H.S. (2008), "Robustness of composite floor systems with shear connections: modeling, simulation, and evaluation", *J. Struct. Eng.*, **134**(11), 1717-1725. https://doi.org/10.1061/(ASCE)0733-9445(2008)134:11(1717).

Sadek, F., *et al*. (2010), "An experimental and computational study of steel moment connections under a column removal scenario", NIST Technical Note 1669, National Institute of Standards and Technology, Gaithersburg, MD.

Shahabi, S.E.M., Sulong, N.H.R. and Shariati, M. (2016), "Performance of shear connectors at elevated temperatures-A review", *Steel Compos. Struct.*, **20**(1), 185-203. https://doi.org/10.12989/scs.2016.20.1.185.

Sun, R.R., Huang, Z.H. and Burgess, I. (2012), "Progressive collapse analysis of steel structures under fire conditions", *Eng. Struct.*, **34**, 400-413. https://doi.org/10.1016/j.engstruct.2011.10.009.

Stevens, D., *et al*. (2011), "DoD Research and Criteria for the Design of Buildings to Resist Progressive Collapse", *J. Struct. Eng.*, **137**(9), 870-880. https://doi.org/10.1061/(ASCE)ST.1943-541X.0000432.

Tian, L.M., *et al*. (2017), "Dynamic analysis method for the progressive collapse of long-span spatial grid structures", *Steel Compos. Struct.*, **23**(4), 435-444. https://doi.org/10.12989/scs.2017.23.4.435.

Wald F., Sokol Z. and Moore D. (2009), "Horizontal forces in steel structures rested in fire", *J. Constr. Steel. Res.*, **65**, 1896-1903. https://doi.org/10.1016/j.jcsr.2009.04.020.

Ye, Z.N., *et al*. (2019), "Experimental study on cyclically-

damaged steel-concrete composite joints subjected to fire", *Steel Compos. Struct.*, **30**(4), 351-364. https://doi.org/10.12989/scs.2019.30.4.351.

Yu, M., Zha, X.X. and Ye, J.Q. (2010), "The influence of joints and composite floor slabs on effective tying of steel structures in preventing progressive collapse", *J. Constr. Steel. Res.*, **66**, 442-451. https://doi.org/10.1016/j.jcsr.2009.10.008.

DL